Biochimica et Biophysica Acta 1788 (2009) 2594–2602

Contents lists available at ScienceDirect

Biochimica et Biophysica Acta

journal homepage: www.elsevier.com/locate/bbamem

Substrate discrimination by ergothioneine transporter *SLC22A4* and carnitine transporter *SLC22A5*: Gain-of-function by interchange of selected amino acids

Petra Bacher, Susanne Giersiefer, Markus Bach, Christian Fork, Edgar Schömig, Dirk Gründemann *

Department of Pharmacology, University of Cologne, Gleueler Straβe 24, 50931 Cologne, Germany

ARTICLE INFO

Article history:
Received 19 August 2009
Received in revised form 23 September 2009
Accepted 28 September 2009
Available online 6 October 2009

Keywords:
Carnitine transporter
Ergothioneine transporter
Gain-of-function
Site-directed mutagenesis
Substrate discrimination

ABSTRACT

ETT (originally designated as OCTN1; human gene symbol *SLC22A4*) and CTT (OCTN2; *SLC22A5*) are highly specific transporters of ergothioneine and carnitine, respectively. Despite a high degree of sequence homology, both carriers discriminate precisely between substrates: ETT does not transport carnitine, and CTT does not transport ergothioneine. Our aim was to turn ETT into a transporter for carnitine and CTT into a transporter for ergothioneine by a limited number of point mutations. From a multiple alignment of several mammalian amino acid sequences, those positions were selected for conversion that were momentously different between ETT and CTT from human but conserved among all orthologues. Mutants were expressed in 293 cells and assayed for transport of ergothioneine and carnitine. Several ETT mutants clearly catalyzed transport of carnitine, up to 35% relative to wild-type CTT. Amazingly, complementary substitutions in CTT did not provoke transport activity for ergothioneine. In similar contrast, carnitine transport by CTT mutants was abolished by very few substitutions, whereas ergothioneine transport by ETT mutants was maintained even with the construct most active in carnitine transport. To explain these results, we propose that ETT and CTT use dissimilar pathways for conformational change, in addition to incongruent substrate binding sites. In other words, carnitine is excluded from ETT by binding, and ergothioneine is excluded from CTT by turnover movement. Our data indicate amino acids critical for substrate discrimination not only in transmembrane segments 5, 7, 8, and 10, but also in segments 9 and 12 which were hitherto considered as unimportant.

1. Introduction

Based on the analysis of transport efficiency, we have recently established that the transport proteins originally designated as novel organic cation transporters OCTN1 (human gene symbol *SLC22A4*) and OCTN2 (*SLC22A5*) are in fact highly specific transporters of ergothioneine (ET) and carnitine (CT), respectively [1–3]. We thus have introduced previously the functional names ETT and CTT. An alignment and comparison of amino acid sequences indicates that ETT and CTT, e.g., from human are very closely related, with 77% identity and 82% similarity. In other words, out of 551 or 557 amino acids, respectively, only 133 positions are unequal. Despite the high degree of sequence homology, both carriers discriminate precisely between ET and CT: ETT does not transport CT, and CTT does not transport ET [1,3].

ET and CT contain some common structural elements (Fig. 1), so the substrate binding surfaces likely are identical in some parts. Since Na^+ drives uptake with both carrier types, this may be true, for example, for the sodium binding site. However, in order to achieve specificity, other parts must be different. Obviously, substrate discrimination is entirely determined by the 133 positions with unequal amino acids. We expect that many of these differences are irrelevant for substrate discrimination (evolutionary noise [4]); thus, only a small subset of the 133 positions with unequal amino acids may be responsible for substrate discrimination.

The aim of the present study was to turn ETT into a transporter for CT and CTT into a transporter for ET by a limited number of point mutations. Such a gain-of-function conversion presents an outstanding opportunity to identify the amino acids that determine substrate discrimination in integral membrane transport proteins.

2. Materials and methods

2.1. Plasmid constructs

The cDNAs of ETT from human (ETTh) and CTT from human (CTTh) were available from previous studies [1]. For easy generation and combination of mutations, each transporter was divided into 4 parts. Fragments with *Esp*3I, *Bsp*QI, or *Nco*I restriction sites at the ends were generated by PCR and cloned into pUC19. Mutations were generated with the QuikChange® II Kit (Stratagene, Agilent Technologies, Waldbronn, Germany); all inserts were fully sequenced to verify the

Abbreviations: CT, carnitine; CTT, carnitine transporter; ET, ergothioneine; ETT, ergothioneine transporter; LC, liquid chromatography; MPP^+, 1-methyl-4-phenylpyridinium; MS, mass spectrometry; TMS, transmembrane segment

* Corresponding author. Tel.: +49 0221 478 7455; fax: +49 0221 478 5022.
E-mail address: dirk.gruendemann@uni-koeln.de (D. Gründemann).

0005-2736/$ – see front matter © 2009 Elsevier B.V. All rights reserved.
doi:10.1016/j.bbamem.2009.09.019

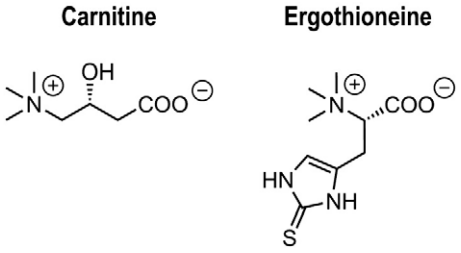

Fig. 1. Structures of L-carnitine (CT) and L-ergothioneine (ET).

desired alteration and the absence of unwanted mutations. The 4 fragments plus an eGFP fragment were ligated into expression vector pEBTetD [5] that had been modified in the polylinker between the *Hin*dIII and *Not*I sites. For wild-type and mutant ETTh plasmids, the 5′-interface between pEBTetD and cDNA is **GTTTAAACTTAAGCTT** gccacc ATGCGGGACTACGAC (plasmid polylinker in bold, Kozak motif lowercase, cDNA underlined); the interface between ETTh and eGFP (in italics) is AGGTTCTAATAACTGCATTC tcc *ATGGTGAGCAAGGGCGAG*; and the interface of eGFP and polylinker is *GAGCTGTACAAGTAA* a **GCGGCCGCGGG**. For wild-type and mutant CTTh plasmids, the 5′-interface between pEBTetD and cDNA is **GTTTAAACTTAAGCTT** gccacc ATGCGGGACTACGAC; the interface between CTTh and eGFP is TCCTTAAAAGCACAGCCTTC tcc *ATGGTGAGCAAGGGCGAG*; and the interface of eGFP and polylinker is as above. Finally, the entire transporter open reading frame of all assembled mutants was sequenced for verification.

2.2. Cell culture

293 cells (ATCC CRL-1573; also known as HEK-293 cells), a transformed cell line derived from human embryonic kidney, were grown at 37 °C in a humidified atmosphere (5% CO_2) in plastic culture flasks (Falcon 3112, Becton Dickinson, Heidelberg, Germany). The growth medium was Dulbecco's modified Eagle medium (Life Technologies 31885-023, Invitrogen, Karlsruhe, Germany) supplemented with 10% fetal calf serum (PAA Laboratories, Cölbe, Germany). Medium was changed every 2–3 days and the culture was split every 5 days.

Stably transfected cell lines were generated as reported previously [5]; cell culture medium always contained 3 μg/ml puromycin (PAA Laboratories) to ascertain plasmid maintenance. To turn on protein expression, cells were cultivated for at least 20 h in regular growth medium supplemented with 1 μg/ml doxycycline (195044, MP Biomedicals, Eschwege, Germany).

2.3. Transport assays

For measurement of solute uptake, cells were grown in surface culture on 60-mm polystyrol dishes (Nunclon 150288, Nunc, Roskilde, Denmark) precoated with 0.1 g/l poly-L-ornithine in 0.15 M boric acid–NaOH, pH 8.4. Cells were used for uptake experiments at a confluence of at least 70%. Uptake was measured at 37 °C. Uptake buffer contains 125 mmol/l NaCl, 25 mmol/l HEPES–NaOH pH 7.4, 5.6 mmol/l (+)glucose, 4.8 mmol/l KCl, 1.2 mmol/l KH_2PO_4, 1.2 mmol/l $CaCl_2$, and 1.2 mmol/l $MgSO_4$. After preincubation for at least 20 min in 4 ml of uptake buffer, the buffer was replaced with 2 ml of substrate in uptake buffer. The total substrate concentration if not indicated otherwise was 0.1 μmol/l for radiotracer assays (^{3}H-carnitine) and 10 μmol/l for unlabeled compounds (ET). Incubation was stopped after 1 min by rinsing the cells four times each with 4 ml ice-cold uptake buffer. Radioactivity was determined, after cell lysis with 0.1% vol./vol. Triton X-100 in 5 mmol/l TRIS–HCl pH 7.4, by liquid scintillation counting. For LC-electrospray ionization-MS/MS analysis, the cells were lysed with 4 mmol/l $HClO_4$ and stored at −20 °C. After centrifugation (1 min, 16,000×*g*, 20 °C) of thawed lysates, 100 μl of the supernatant was mixed with 10 μl unlabeled MPP^+ iodide (0.5 ng/μl) which served as internal standard. Of this mixture, 20 μl samples were analyzed by LC-MS/MS (flow rate 250 μl/min) on a triple quadrupole mass spectrometer (4000 Q TRAP, Applied Biosystems, Darmstadt, Germany). Atmospheric pressure ionization with positive electrospray was used. Isocratic chromatography (70% methanol and 30% 0.1% formic acid) was employed with a Waters Atlantis HILIC silica column (length 50 mm, diameter 3 mm, particle size 5 μm). For quantification (scan time 150 ms), the optimal collision energy for argon-induced fragmentation in the second quadrupole was determined for each analyte. From the product ion spectra, the following fragmentations were selected for selected reaction monitoring (m/z parent, m/z fragment, collision energy): ergothioneine: 230, 127, 27 V; MPP^+: 170, 128, 43 V. For each analyte, the area of the intensity vs. time peak was integrated and divided by the area of the MPP^+ peak to yield the analyte response ratio. Linear calibration curves were constructed from at least six standards which were prepared using control cell lysates as solvent. Sample analyte content was calculated from the analyte response ratio and the slope of the calibration curve, obtained by linear regression.

Protein was measured by the BCA assay (Pierce) with bovine serum albumin as standard. The protein content of MS samples was estimated from 3 matched cell dishes.

2.4. Calculations and statistics

The clearance equals initial rate of specific uptake (=uptake mediated by expressed carrier) divided by substrate concentration; it is directly proportional to k_{cat}/K_m (k_{cat}: turnover number) and thus a valid measure of efficiency of transport (provided that the substrate concentration is much smaller than the respective K_m) [6,7]. Specific uptake equals total uptake minus uptake into control cells (=non-specific uptake).

Analysis of saturation curves has been reported previously [8]. K_m values are given as geometric mean with 95% confidence interval. In the figures, symbols and bars represent arithmetic mean ± SEM ($n=3$) if not indicated otherwise in the legend.

2.5. Chemicals

Unlabeled compounds were as follows: L-carnitine (C-0283, Sigma-Aldrich, Munich, Germany), L-ergothioneine (F-3455, Bachem, Bubendorf, Switzerland), 1-methyl-4-phenylpyridinium iodide (D-048, Sigma-Aldrich). All other chemicals were at least of analytical grade. Radiotracer: L-carnitine hydrochloride (H-3, 3.1 kBq/pmol, ART-293, ARC, St. Louis, MO, USA).

3. Results

3.1. Strategy of selection of substitutions

All substitutions were simply made according to the alignment of the amino acid sequences of ETT from human (ETTh) and CTT from human (CTTh) (Supplementary Fig. 1). Since it is not feasible to create and analyze all possible combinations of all 133 transitions, the challenge was to select what might be relevant substitutions. We used evolutionary conservation as our prime indicator of relevance. Although ETT and CTT apparently are present in vertebrates in general (e.g., birds, reptiles, and fishes), we included, for a high level of basic similarity, only mammalian orthologues in evolutionary analysis. Thus, a multiple alignment of the amino acid sequences of ETT and CTT from human, pig, cattle, dog, mouse, and rat was generated (Supplementary Fig. 1). We then selected those positions that were strikingly different between ETTh and CTTh, but conserved

among all orthologues. Since according to these criteria none of the first 230 positions qualified, no substitutions at all were made in this high similarity region.

3.2. ETTh mutants—carnitine transport

The first set of ETTh mutants contained substitutions in transmembrane segments (TMS) 5, 7, 10, and 11. Most of these we consider as potentially momentous: removal or addition of a hydroxyl group (T ⟺ I, L ⟺ T, F ⟺ Y, A ⟺ S), aromatic side chain (V ⟺ F), or glycine (A ⟺ G). All mutants are specified in Table 1. In order to keep the number of constructs manageable, we have grouped together substitutions from the same TMS.

All constructs contained eGFP at the C-terminus in order to verify uniform membrane trafficking. Our experience (unpublished data) suggests that such an attachment has no influence on transport activity. All mutants described in this work showed similar expression levels (FACS analysis, data not shown) and membrane localization (fluorescence microscopy; Supplementary Fig. 2) as the respective wild-type carriers. Mutants were generated by site-directed mutagenesis, inserted into our pEBTetD expression vector and stably transfected into 293 cells. pEBTetD is an episomal Epstein–Barr

Table 1
Designation and definition of mutants.

#	1	2	3	4	5	6	7	8	9	10	11	12	13	14	15	16	17	18	19	20	21	22	23	
TMS	5	5	5	6	7	7	7	7	8	9	9	9	9	9L10	9L10	10	10	11	11	11L12	12	12	12	
wild-type ETTh	T	F	V	P	A	L	T	A	T	I	A	V	G	Y	I	L	F	A	A	N	V	I	G	
Position	237	239	241	272	339	351	352	358	387	400	403	404	410	422	427	444	447	460	475	485	498	500	501	
wild-type CTTh	I	Y	F	A	R	T	I	G	L	S	T	A	S	L	T	V	Y	G	S	D	I	T	A	
Position	237	239	241	272	341	353	354	360	389	402	405	406	412	424	429	446	449	462	477	487	500	502	503	
Mutant designation																								#
e5	■	■	■																					1
c5a	▒																							2
c5b		▒	▒																					3
e7						■	■																	4
c7						▒	▒																	5
c9										▒	▒	▒	▒											6
e10																■	■							7
c10																▒	▒							8
e11																		■	■					9
c11																		▒	▒					10
c12a																						▒	▒	11
e7.10						■	■									■	■							12
e7a.10					■	■	■	■								■	■							13
c5b.11		▒	▒															▒	▒					14
c7a.10					▒	▒	▒	▒								▒	▒							15
c9.12a										▒	▒	▒	▒									▒	▒	16
e5.7.10	■	■	■			■	■									■	■							17
c5.7a.10	▒	▒	▒		▒	▒	▒	▒								▒	▒							18
c7a.8.10					▒	▒	▒	▒	▒							▒	▒							19
c7a.9.10					▒	▒	▒	▒		▒	▒	▒	▒			▒	▒							20
c7a.10.11					▒	▒	▒	▒								▒	▒	▒	▒					21
c7a.10.12a					▒	▒	▒	▒								▒	▒					▒	▒	22
e5.6.7.10	■	■	■	■		■	■									■	■							23
e5.7.8.10	■	■	■			■	■		■							■	■							24
c5.7a.8.10.11.12a	▒	▒	▒		▒	▒	▒	▒	▒							▒	▒	▒	▒			▒	▒	25
c5.7a.8.9.10.11.12a	▒	▒	▒		▒	▒	▒	▒	▒	▒	▒	▒	▒			▒	▒	▒	▒			▒	▒	26
e5.7.9.10	■	■	■			■	■			■	■	■	■			■	■							27
e5.7.10.12	■	■	■			■	■									■	■				■	■	■	28
e5.7.8.9.10	■	■	■			■	■		■	■	■	■	■			■	■							29
e5.7.9.10.12	■	■	■			■	■			■	■	■	■			■	■				■	■	■	30
e5.7.8.9.10.12	■	■	■			■	■		■	■	■	■	■			■	■				■	■	■	31
c5.7a.8.9.10.12a	▒	▒	▒		▒	▒	▒	▒	▒	▒	▒	▒	▒			▒	▒					▒	▒	32
eA						■	■							■	■	■	■							33
eB	■	■	■			■	■									■	■			■	■	■	■	34
eC	■	■	■	■	■	■	■	■	■	■	■	■	■	■	■	■	■	■	■	■	■	■	■	35

Black boxes indicate mutants ("e") based on wild-type ETTh, and gray boxes mark mutants ("c") based on wild-type CTTh. A capital "L" in row TMS (transmembrane segment) indicates an amino acid in a loop.

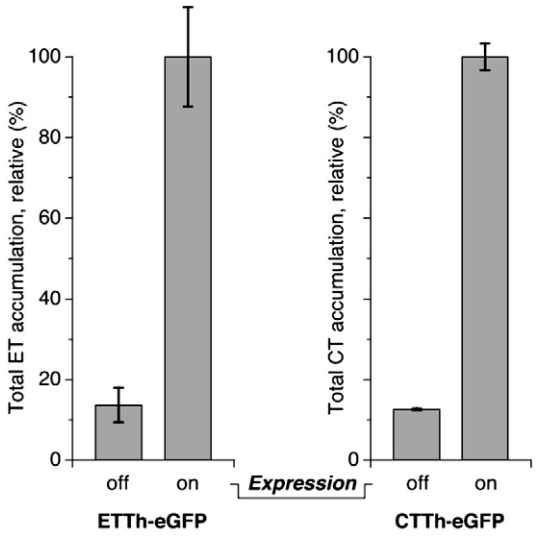

Fig. 2. Signal-to-noise in transport assays with wild-type ETTh or CTTh. 293 cells were stably transfected with either pEBTetD/ETTh-eGFP or pEBTetD/CTTh-eGFP. Expression of transporter cDNA was turned on by addition of doxycycline. Cells grown in dishes were incubated for 1 min with substrate (3.3 μmol/l unlabeled ET or 1.0 μmol/l ^{3}H-CT) in uptake buffer and then processed as described in Materials and methods. On-state accumulation (=100%) corresponded to 103±13 pmol min^{-1} mg protein^{-1} for ETTh, and 61±2 pmol min^{-1} mg protein^{-1} for CTTh. Note that endogenous ET (accumulated during cell culture from calf serum; 28±7 pmol mg protein^{-1} for off-state cells and 62±1 pmol mg protein^{-1} for on-state cells) was determined with paired dishes by incubation in uptake buffer without ET and subtracted.

plasmid vector for doxycycline-inducible protein expression in human cell lines based on the simple tetracycline repressor [5]. As there is no integration of vector into the genome, clonal isolation of transfected cells is not necessary; we thus use cell pools rather than single cell clones. Expression is turned on by addition of 1 μg/ml doxycycline to the culture medium for about 20 h. With, e.g., ETTh, this system provides a high rate of carrier-mediated transport in the on-state (=100%) and a low rate (4%) in the off-state (=leak expression) [5]. The data shown in Fig. 2 validate sufficient signal over background: carnitine uptake mediated by exogenous wild-type CTTh was much higher than nonspecific accumulation due to diffusion, binding, endogenous CTTh [1], and leak expression of CTTh.

Fig. 3 shows initial rates of uptake of ^{3}H-carnitine of the first set of mutants relative to wild-type CTTh (100%). Background accumulation was estimated with wild-type ETTh and subtracted from all rates. Both controls were always transfected and measured in parallel.

Mutations only within a single TMS were virtually without effect on uptake of carnitine (Fig. 3a). However, the combination of changes in TMS 7 and 10 (mutant e7.10) clearly promoted uptake of carnitine (8.8% relative to CTTh). A further substantial increase to 15.7% was achieved with mutant e5.7.10 (Fig 3b). Surprisingly, the substitutions in TMS 11 reduced carnitine transport.

In the second set of ETTh mutants, additional substitutions in TMS 6, 8, 9, and 12 were added to mutant e5.7.10. The changes in TMS 8 and particularly in 9 and 12 further increased carnitine transport (Fig. 4a). Again, more prominent increases were seen with combinations of the mutated segments; the highest rate was achieved by construct e5.7.8.9.10.12 which displayed 35% of wild-type CTTh carnitine transport activity (Fig. 4b). By contrast, the change in TMS 6 reduced transport activity (Fig. 4a).

A decrease in carnitine transport relative to the respective reference construct was also observed with 3 mutants with additional substitutions (cf., Table 1): mutant e7a.10 (7.5±0.4%) which is e7.10 (10.8±0.8%) plus 2 further changes in TMS 7, mutant eA (5.5±0.5%) which is e7.10 (10.8±0.8%) plus 2 further changes in the external loop between TMS 9 and 10, and mutant eB (14.5±3.9%) which is e5.7.10.12 (18.6±4.5%) plus 1 further change in the external loop between TMS 11 and 12. Finally, mutant eC (7.3±0.4%), which contains all 23 mutations from Table 1, was much less active than our best mutant e5.7.8.9.10.12 with 15 changes (34.7±4.2%).

3.3. ETTh mutants—ergothioneine transport

The mutants that had shown a progressive increase of carnitine transport were also assayed for ET transport. Paired dishes were used to measure uptake of carnitine (described above) and ET under

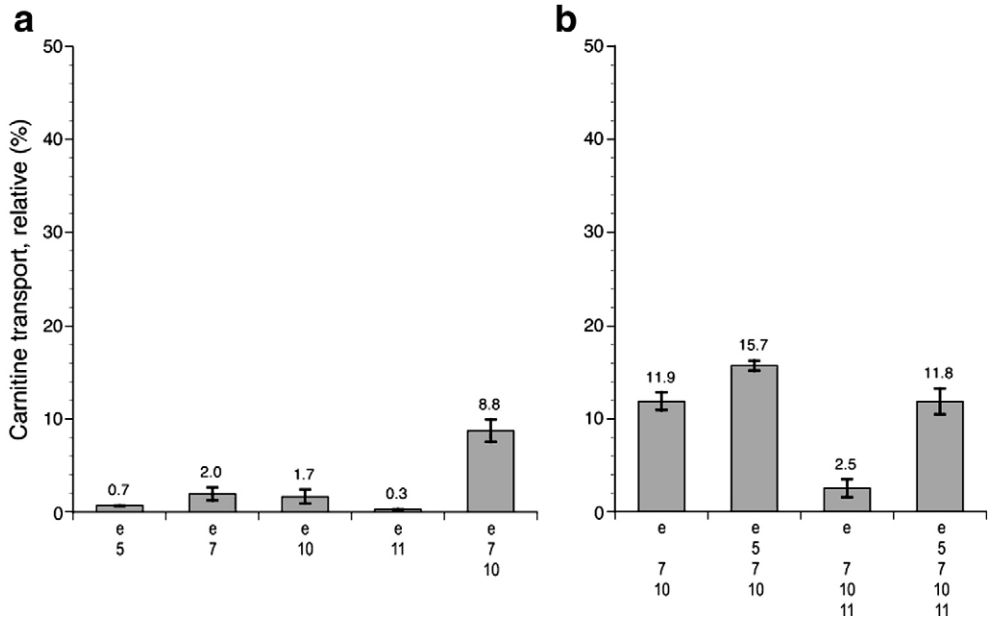

Fig. 3. Carnitine transport activity of ETTh mutants (first set) relative to wild-type CTTh. Initial rates of uptake of ^{3}H-carnitine (0.1 μmol/l; 1 min) were determined with stably transfected 293 cells. Shown is mean±SEM (n=2–3, assays performed on different days). Accumulation by wild-type ETTh was subtracted from all rates. Positive (wild-type CTTh-eGFP; average (n=12) CT accumulation 12.8±0.9 pmol min^{-1} mg protein^{-1}) and negative control cells (wild-type ETTh-eGFP, 0.52±0.03 pmol min^{-1} mg protein^{-1}) were always transfected and assayed in parallel.

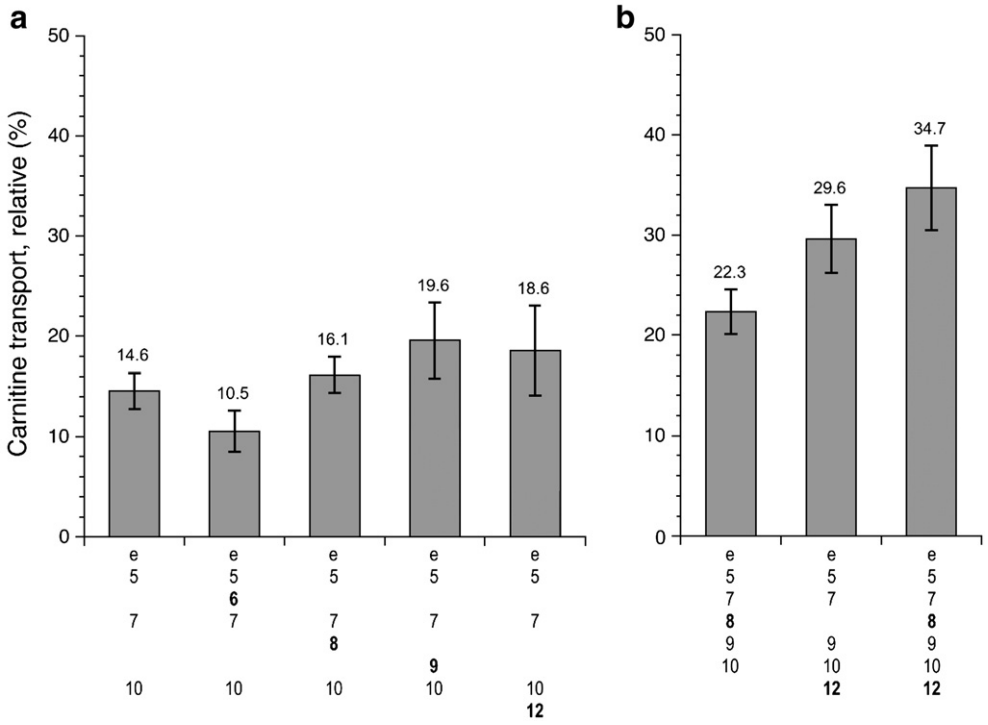

Fig. 4. Carnitine transport activity of ETTh mutants (second set) relative to wild-type CTTh. See legend to Fig. 3 for experimental conditions.

identical conditions of protein expression. Cells were incubated 1 min with ET (10 μmol/l in uptake buffer), and then the ET content was measured by LC-MS/MS. The initial endogenous ET content was estimated and subtracted separately for each cell line with paired dishes that were incubated with uptake buffer without ET. Note that this simple approach, which reduces the number of dishes over the precise method [2] by 50%, yields the sum of specific (catalyzed by the exogenous transporter) and nonspecific accumulation. Yet this sum overestimates true exogenous ET transport activity only very slightly here, since 293 cells do not express endogenous ETTh [3], and since nonspecific uptake of ET is very low. Uptake mediated by exogenous ETTh was much higher than nonspecific background accumulation of ET due to diffusion, binding, and leak expression of ETTh (Fig. 2).

Fig. 5 shows accumulation of ET relative to wild-type ETTh (100%). Surprisingly, efficiency of transport of ET was fully maintained or even clearly increased for all mutants except eC, the all-substitutions construct, which was only at 40.2 ± 5.3% relative to wild-type. Thus, the increase in CT transport (Figs. 3 and 4) does not correlate with a decrease in ET transport.

3.4. ETTh mutants—substrate affinity

Substitutions may affect substrate binding (K_m) or turnover ($k_{cat} = V_{max} / T_{total}$). Mutations that improve binding of substrate to the carrier should increase affinity, i.e., decrease the K_m value. Saturation of transport of carnitine was determined with selected mutants (Table 2); note that because of the poor signal-to-noise ratio, we have not analyzed wild-type ETTh here. The results indicate that increased carnitine transport as described above correlates well with increased affinity: mutant e5.7.8.9.10.12 (K_m = 98 μmol/l) has 3-fold higher affinity than mutant e5.7.10 (280 μmol/l). However, the affinity of wild-type CTTh is still 7-fold higher (15 μmol/l). A relatively strong increase in affinity was imparted by the changes in TMS 9.

Saturation of transport of ET was analyzed with mutant e5.7.8.9.10.12 to see whether this mutant—profoundly altered, but with full transport efficiency for ET (Fig. 5)—still had the original affinity. Our results (Fig. 6) indicate markedly reduced affinity (66 μmol/l; 95% confidence interval (95% CI), 48–90 μmol/l) vs. wild-type ETTh (16 μmol/l; 95% CI, 12–22 μmol/l). Since here both cell lines were transfected and analyzed in parallel, a comparison of V_{max}/K_m is possible. With virtually identical numbers (30.0 vs. 31.9 μl min^{-1} mg $protein^{-1}$), it can be concluded that the mutant has a 4-fold higher turnover number than wild-type ETTh.

3.5. CTTh mutants—ergothioneine transport

A set of CTTh mutants was created analogous to the ETTh mutants (see Table 1 for designations and exact descriptions). Again, all constructs contained eGFP at the C-terminus, and all mutants showed expression levels (FACS analysis, data not shown) and membrane localization (fluorescence microscopy; Supplementary Fig. 2b) like the wild-type carriers. Accumulation of ET, measured by LC-MS/MS as above, was not consistently increased over wild-type CTTh for any of the examined mutants (each assayed 2 or 3 times on different days; data not shown). Mutants c9, c12a, c9.12a, and c7a.9.10 were not analyzed here.

Table 2
Affinity for carnitine of selected ETTh mutants.

Mutant	K_m (μmol/l)	95% CI	V_{max} (nmol min^{-1} mg $protein^{-1}$)
CTTh wild-type	15	11–21	1.08 ± 0.04
e5.7.10	280	220–360	1.94 ± 0.09
e5.7.8.10	230	210–270	2.08 ± 0.04
e5.7.9.10	140	90–200	1.68 ± 0.10
e5.7.10.12	210	140–320	1.72 ± 0.12
e5.7.8.9.10	140	110–180	2.66 ± 0.11
e5.7.8.9.10.12	98	68–140	1.72 ± 0.08

Given is the K_m with the corresponding 95% confidence interval (CI) and the V_{max} with corresponding SD measured by saturation of uptake of ^{3}H-carnitine (n = 18). Note that the different mutants were not measured in parallel; hence, V_{max}/K_m cannot be compared.

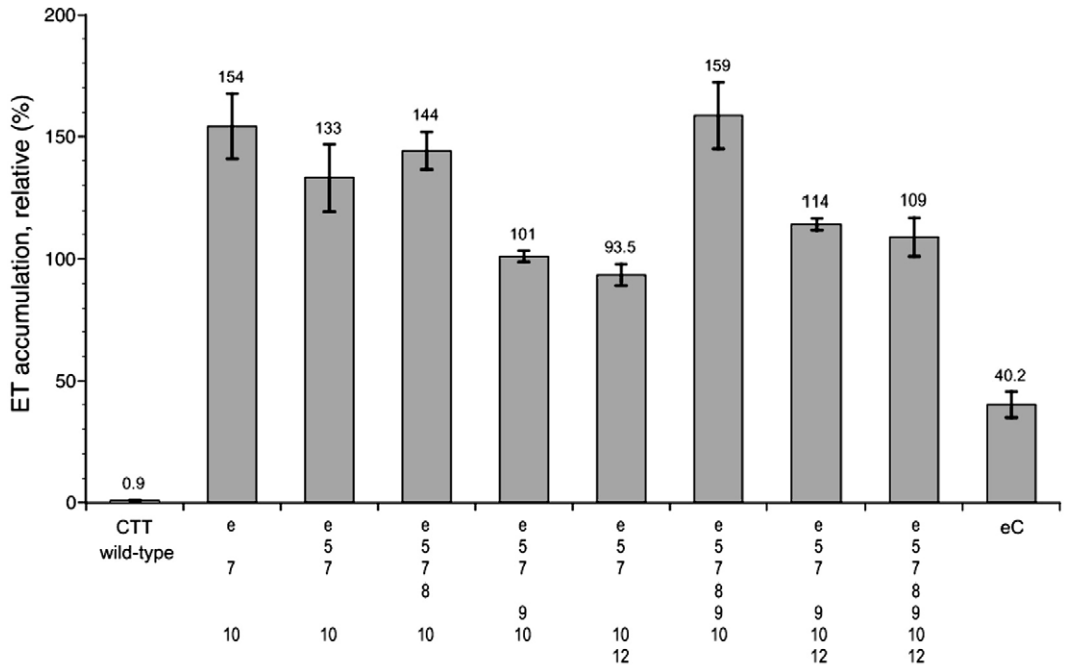

Fig. 5. Ergothioneine transport activity of ETTh mutants relative to wild-type ETTh. Initial rates of uptake of unlabeled ET (10 μmol/l; 1 min) were determined with stably transfected 293 cells. Shown is mean ± SEM ($n = 2–3$, assays performed on different days). For each cell line, endogenous ET (accumulated during cell culture from FCS) was measured in parallel by incubation in uptake buffer without ET and subtracted. Positive (wild-type ETTh-eGFP; average ($n = 14$) ET accumulation 770 ± 90 pmol min^{-1} mg $protein^{-1}$) and negative control cells (wild-type CTTh-eGFP, 7 ± 1 pmol min^{-1} mg $protein^{-1}$) were always transfected and assayed in parallel.

3.6. CTTh mutants—carnitine transport

Fig. 7 shows initial rates of uptake of ^{3}H-carnitine of all CTTh mutants relative to wild-type CTTh (100%). As for the ETTh mutants, background accumulation was estimated with wild-type ETTh and subtracted from all rates. Both controls were always transfected and measured in parallel. Each mutant was assayed 2 or 3 times on different days.

By contrast to the ETTh mutants described above, a marked loss-of-function was achieved easily by 1 to 4 amino acid substitutions within a single TMS (Fig. 7a). Changes in TMS 5 or 7 caused a strong reduction of carnitine transport, and changes in TMS 10, 12, or 9 a moderate reduction. The changes in TMS 11 had no effect.

The combination c7a.10 was used as reference for further constructs (Fig. 7b). Additional changes in either TMS 9 or TMS 12 had no effect. However, additional changes in TMS 5 generated totally inactive mutants (c5.7a.10 and 3 further mutants that contain this set). Surprisingly, addition of changes in TMS 8 and particularly in TMS 11 to c7a.10 increased transport of carnitine. Analogously, mutant c5b.11 showed much higher transport than c5b. By contrast, transport by mutant c9.12a (37.1%) was clearly reduced compared to the corresponding base mutants c9 (82.9%) and c12a (51.3%).

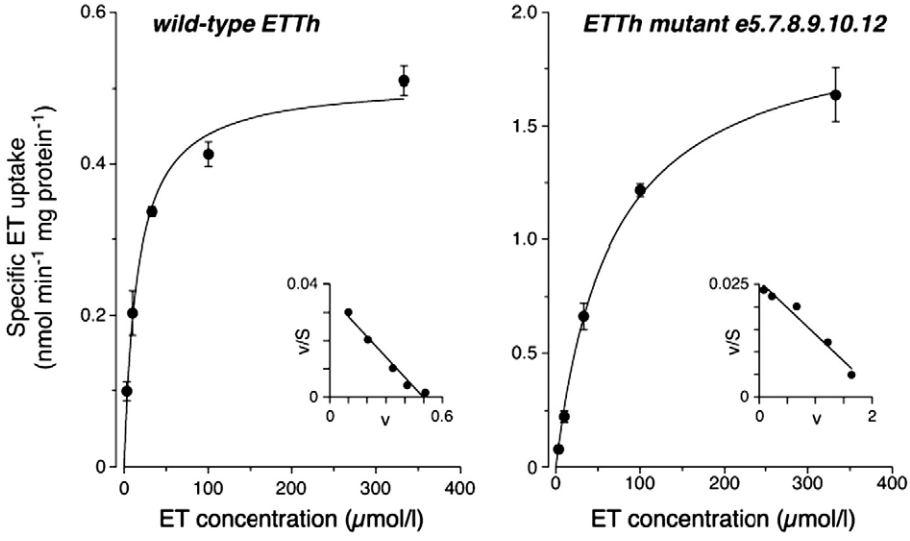

Fig. 6. Saturation of uptake of ET mediated by wild-type ETTh and ETTh mutant e5.7.8.9.10.12. An uptake period of 1 min was chosen to approximate initial rates of transport. Shown is mean ± SEM ($n = 3$). Specific uptake equals total content minus endogenous content divided by uptake time minus nonspecific uptake. Nonspecific uptake with wild-type ETTh cells increased linearly with ET concentration, slope = 0.18 μl min^{-1} mg $protein^{-1}$. V_{max} = 0.51 ± 0.02 (wild-type) or 2.0 ± 0.1 nmol min^{-1} mg $protein^{-1}$. Insets: Eadie–Scatchard transformation.

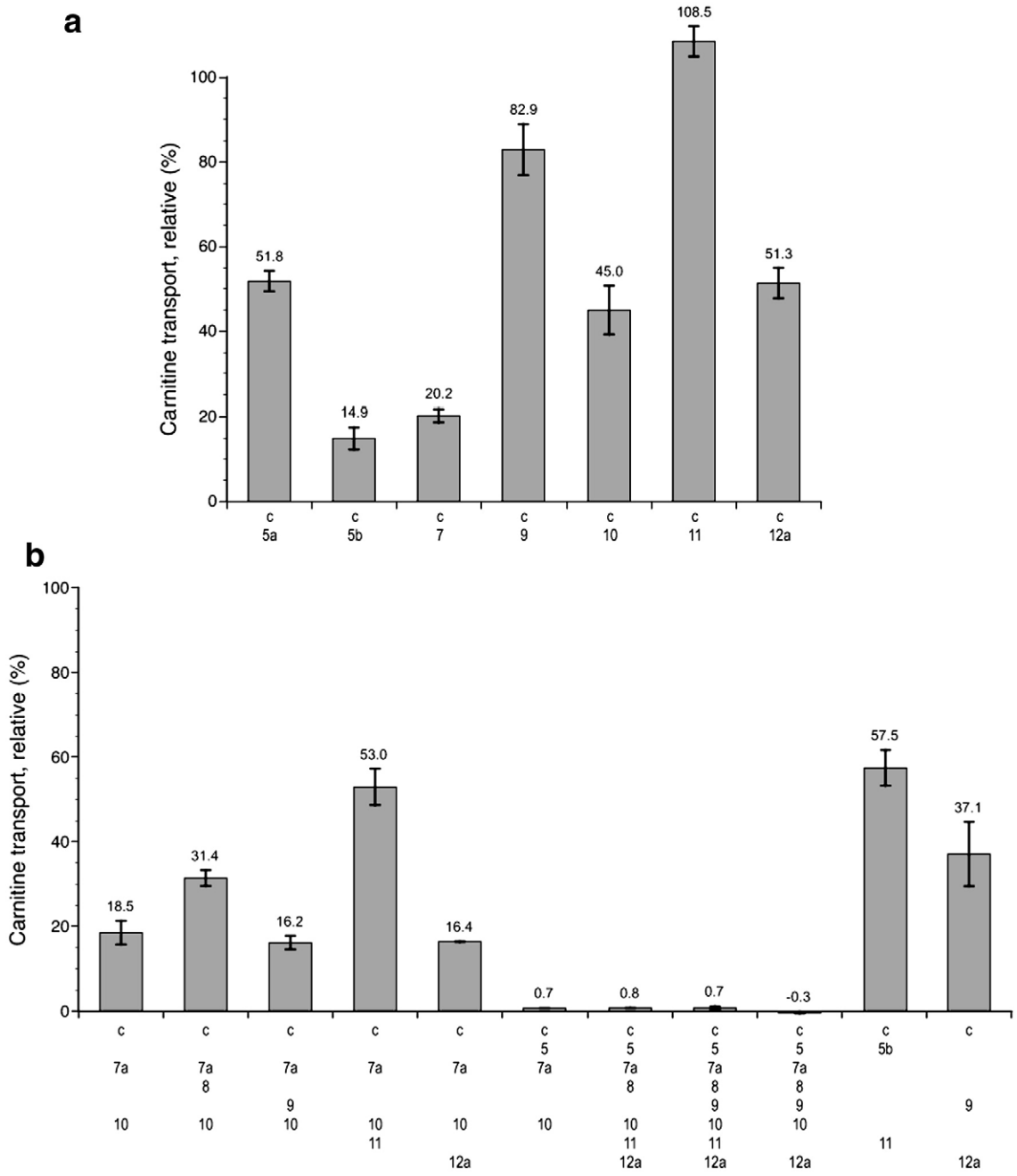

Fig. 7. Carnitine transport activity of CTTh mutants relative to wild-type CTTh. Initial rates of uptake of ^{3}H-carnitine (0.1 μmol/l; 1 min) were determined with stably transfected 293 cells. Shown is mean ± SEM (n = 2–3, assays performed on different days). Accumulation by wild-type ETTh was subtracted from all rates. Positive (wild-type CTTh-eGFP; average (n = 9) CT accumulation 13 ± 3 pmol min^{-1} mg protein^{-1}) and negative control cells (wild-type ETTh-eGFP, 0.7 ± 0.2 pmol min^{-1} mg protein^{-1}) were always transfected and assayed in parallel.

4. Discussion

The aim of the present work was to alter the substrate specificity of an integral membrane transport protein. To accomplish such a gain-of-function is a much greater challenge than to delete function—the latter can easily be achieved by a myriad of single amino acid substitutions. Point mutations were selected based on potentially momentous differences in the evolutionary analysis of mammalian orthologues of ETT and CTT (Supplementary Fig. 1). We have indeed succeeded to impart a high rate of carnitine transport—35% relative to the wild-type carnitine transporter (Fig. 4b)—to ETT, a carrier that originally totally rejects CT as substrate. Note that Amat di San Filippo et al. [9] have reported transport of carnitine for a chimeric construct where amino acids 1–193 of ETTh replaced the corresponding part of CTTh at only about 50% relative to wild-type CTTh. Hence, since we have not made any changes in this region, we could only expect to achieve this much; our mutant e5.7.8.9.10.12 comes impressively close to this mark.

Our results establish that substrate discrimination is based on multiple positions distributed to at least 6 transmembrane segments: 5, 7, 8, 9, 10, and 12. Note that further contacts to substrate can be expected among those amino acids that are identical in ETT and CTT [10–14], but these do not contribute to discrimination. Our results agree with reports about other *SLC22* carriers and the glucose transporter GLUT1 (which belongs to the same superfamily) where residues critical for transport activity were found in TMS 5 [15,16],

TMS 7 [16–19], TMS 8 [19–21], and TMS 10 [16,22–24]. In the previous study with ETT–CTT–chimera mentioned above [9], 2 regions essential for carnitine transport were identified (CTT sequence numbering): 341–453 (containing TMS 7–10) and 454–557 (TMS 11–12); further contacts to substrate were postulated between 194 and 340 (TMS 4–6). This basically agrees with our results. However, our TMS-based approach provides higher resolution and thus more differentiated insight: for example, our data suggest that changes in TMS 12 affect substrate affinity (Table 2); by contrast, the 454–557 (TMS 11–12) replacement [9] reduced V_{max}, but did not alter K_m. Moreover, only transport of carnitine was analyzed then since ET was unknown as physiological substrate of ETT at the time. It is quite remarkable that our best construct, e5.7.8.9.10.12, contains only 15 amino acid changes; since we have grouped potentially relevant substitutions in TMS and not tested each mutation individually, the minimum number needed for the same level of function might even be lower. Increased carnitine transport correlates well with increased affinity (Table 2).

Amazingly, complementary substitutions in CTT could not provoke any transport activity for ET whatsoever. In similar contrast, CT transport by CTT mutants was easily abolished by very few substitutions (Fig. 7), whereas ET transport by ETT mutants was fully maintained even with the construct most active in CT transport (Fig. 5). To explain these results, we suggest that ETT and CTT have not only dissimilar substrate binding sites but also dissimilar pathways for conformational change. In other words, some parts of the carriers move differently during turnover. It appears that the ET movement pathway of ETT accomodates CT—a smaller and more flexible molecule (Fig. 1)—well, but the CT movement pathway of CTT cannot accomodate ET. This model suggests that we have sufficiently transformed binding sites to establish CT transport by ETT mutants and to abolish CT transport by CTT mutants. However, we have not exchanged movement pathways: ET is not transported by CTT mutants and is still transported by ETT mutants. From another perspective, CT is excluded from ETT by binding, and ET is excluded from CTT by movement.

We have constructed several ETTh mutants that contain substitutions (Table 1, columns 4, 5 + 8, 9, 14 + 15, 18 + 19, and 20) which clearly reduced carnitine transport. This was contrary to our naive expectation that any additional mutation would either increase CT transport or have no effect. Changes in these positions probably impair the movement pathway ("spanner in the works") and thus reduce rates of transport. From another perspective, a relative reduction of transport presumably indicates a position involved in turnover movement rather than mere substrate binding. In accordance, in the report by Amat di San Filippo et al. [9], mutations (CTT sequence numbering) R341L, L424Y, and T429I (which in our assignment of TMS are located not in, but between transmembrane segments) reduced V_{max}, but did not affect K_m. Further complementary transitions are necessary to establish a different movement pathway. Potential positions (mostly outside the transmembrane segments) are indicated in Supplementary Fig. 1. Of course, we cannot exclude that trivial substitutions (e.g., V ⟺ I) may have an effect.

Several ETTh mutants showed ET transport rates clearly higher than wild-type (Fig. 5). As suggested from Fig. 6, this is most likely caused by a higher turnover number. Similarly, transitions in TMS 8 and 11 increased CT transport by some CTTh mutants (Fig. 7). This suggests that both wild-type carriers operate slower than physically possible. In other words, accurate substrate discrimination is more important than high substrate flux.

ETT and CTT belong to the same superfamily as 3 bacterial carriers with known three-dimensional structures: glycerol-3-phosphate transporter GlpT from *Escherichia coli* [25], lactose permease LacY from *E. coli* [26], and oxalate transporter OxlT from *Oxalobacter formigenes* [27]. It was deduced from these structures that TMS 3, 6, 9, and 12 are not involved in substrate binding or translocation, but—as scaffolding or pillars—encircle and stabilize the inner bundle of the other helices. This notion was fully supported by cysteine-scanning mutagenesis and cysteine reagent accessibility assays of TMS 9 and 12 of GLUT1 [28,29]. However, since our mutant e5.7.10 with about 15% carnitine transport relative to wild-type was still far off the 50% mark, and since our evolutionary analysis indicated interesting positions in TMS 6, 9, and 12, they were included in the second set of ETTh mutants. Indeed, transitions in TMS 9 and 12 clearly promoted uptake of carnitine and increased affinity. It is therefore a major and unexpected finding of the present work that TMS 9 and 12 are not inert, but contribute to substrate discrimination, either by direct binding or by indirectly guiding other segments. These results illustrate that the available bacterial structures can fail to predict precise substrate contacts of *SLC22* transporters. In fact, it is not even possible to generate a reasonable amino acid sequence alignment between the bacterial transporters and ETT or CTT. Moreover, static structures cannot reveal the proposed different movement pathways.

In conclusion, we have managed to impart by point mutations a high rate of carnitine transport to ETT, a carrier that originally totally rejects CT as substrate. Our data indicate amino acids critical for substrate discrimination not only in transmembrane segments 5, 7, 8, and 10 but also in segments 9 and 12 which were hitherto considered as unimportant. We propose that ETT and CTT use dissimilar pathways for conformational change, in addition to dissimilar substrate binding sites, to discriminate substrates.

Acknowledgements

Supported by the Koeln Fortune Program, Faculty of Medicine, University of Cologne (157/2007 and 99/2008). We thank Beatrix Steinrücken, Simone Kalis, and Regina Baucks for skillful technical assistance; Olaf Utermöhlen and coworkers (Institute for Medical Microbiology, Immunology, and Hygiene, University of Cologne) for FACS support; and Hamid Kashkar and coworkers (Institute for Medical Microbiology, Immunology, and Hygiene, University of Cologne) for confocal fluorescence microscopy support.

Appendix A. Supplementary data

Supplementary data associated with this article can be found, in the online version, at doi:10.1016/j.bbamem.2009.09.019.

References

[1] S. Grigat, C. Fork, M. Bach, S. Golz, A. Geerts, E. Schömig, D. Gründemann, The carnitine transporter SLC22A5 is not a general drug transporter, but it efficiently translocates mildronate, Drug Metab. Dispos. 37 (2009) 330–337.
[2] S. Grigat, S. Harlfinger, S. Pal, R. Striebinger, S. Golz, A. Geerts, A. Lazar, E. Schömig, D. Gründemann, Probing the substrate specificity of the ergothioneine transporter with methimazole, hercynine, and organic cations, Biochem. Pharmacol. 74 (2007) 309–316.
[3] D. Gründemann, S. Harlfinger, S. Golz, A. Geerts, A. Lazar, R. Berkels, N. Jung, A. Rubbert, E. Schömig, Discovery of the ergothioneine transporter, Proc. Natl. Acad. Sci. U.S.A. 102 (2005) 5256–5261.
[4] E. Zuckerkandl, Evolutionary processes and evolutionary noise at the molecular level: II. A selectionist model for random fixations in proteins, J. Mol. Evol. 7 (1976) 269–311.
[5] M. Bach, S. Grigat, B. Pawlik, C. Fork, O. Utermöhlen, S. Pal, D. Banczyk, A. Lazar, E. Schömig, D. Gründemann, Fast set-up of doxycycline-inducible protein expression in human cell lines with a single plasmid based on Epstein–Barr virus replication and the simple tetracycline repressor, FEBS J. 274 (2007) 783–790.
[6] D. Gründemann, G. Liebich, N. Kiefer, S. Köster, E. Schömig, Selective substrates for non-neuronal monoamine transporters, Mol. Pharmacol. 56 (1999) 1–10.
[7] E. Schömig, A. Lazar, D. Gründemann, Extraneuronal monoamine transporter and organic cation transporters 1 and 2—a review of transport efficiency, in: H.H. Sitte, M. Freissmuth (Eds.), Handbook of Experimental Pharmacology—Neurotransmitter Transporters, 175, Springer, Heidelberg, 2006, pp. 151–180.
[8] E. Schömig, J. Babin-Ebell, H. Russ, 1,1′-Diethyl-2,2′-cyanine (decynium22) potently inhibits the renal transport of organic cations, Naunyn Schmiedebergs Arch. Pharmacol. 347 (1993) 379–383.
[9] C. Amat di San Filippo, Y. Wang, N. Longo, Functional domains in the carnitine transporter OCTN2, defective in primary carnitine deficiency, J. Biol. Chem. 278 (2003) 47776–47784.

[10] R. Ohashi, I. Tamai, A. Inano, M. Katsura, Y. Sai, J. Nezu, A. Tsuji, Studies on functional sites of organic cation/carnitine transporter OCTN2 (SLC22A5) using a Ser467Cys mutant protein, J. Pharmacol. Exp. Ther. 302 (2002) 1286–1294.
[11] A. Inano, Y. Sai, Y. Kato, I. Tamai, M. Ishiguro, A. Tsuji, Functional regions of organic cation/carnitine transporter OCTN2 (SLC22A5): roles in carnitine recognition, Drug Metab. Pharmacokinet. 19 (2004) 180–189.
[12] P. Seth, X. Wu, W. Huang, F.H. Leibach, V. Ganapathy, Mutations in novel organic cation transporter (OCTN2), an organic cation/carnitine transporter, with differential effects on the organic cation transport function and the carnitine transport function, J. Biol. Chem. 274 (1999) 33388–33392.
[13] K. Lu, H. Nishimori, Y. Nakamura, K. Shima, M. Kuwajima, A missense mutation of mouse OCTN2, a sodium-dependent carnitine cotransporter, in the juvenile visceral steatosis mouse, Biochem. Biophys. Res. Commun. 252 (1998) 590–594.
[14] Z. Rahbeeni, F.M. Vaz, K. Al-Hussein, M.P. Bucknall, J. Ruiter, R.J. Wanders, M.S. Rashed, Identification of two novel mutations in OCTN2 from two Saudi patients with systemic carnitine deficiency, J. Inherit. Metab. Dis. 25 (2002) 363–369.
[15] M. Mueckler, C. Makepeace, Transmembrane segment 5 of the Glut1 glucose transporter is an amphipathic helix that forms part of the sugar permeation pathway, J. Biol. Chem. 274 (1999) 10923–10926.
[16] J.L. Perry, N. Dembla-Rajpal, L.A. Hall, J.B. Pritchard, A three-dimensional model of human organic anion transporter 1: aromatic amino acids required for substrate transport, J. Biol. Chem. 281 (2006) 38071–38079.
[17] M. Hong, F. Zhou, K. Lee, G. You, The putative transmembrane segment 7 of human organic anion transporter hOAT1 dictates transporter substrate binding and stability, J. Pharmacol. Exp. Ther. 320 (2007) 1209–1215.
[18] P.W. Hruz, M.M. Mueckler, Cysteine-scanning mutagenesis of transmembrane segment 7 of the GLUT1 glucose transporter, J. Biol. Chem. 274 (1999) 36176–36180.
[19] B. Feng, Y. Shu, K.M. Giacomini, Role of aromatic transmembrane residues of the organic anion transporter, rOAT3, in substrate recognition, Biochemistry 41 (2002) 8941–8947.
[20] M. Mueckler, C. Makepeace, Analysis of transmembrane segment 8 of the GLUT1 glucose transporter by cysteine-scanning mutagenesis and substituted cysteine accessibility, J. Biol. Chem. 279 (2004) 10494–10499.
[21] B. Feng, M.J. Dresser, Y. Shu, S.J. Johns, K.M. Giacomini, Arginine 454 and lysine 370 are essential for the anion specificity of the organic anion transporter, rOAT3, Biochemistry 40 (2001) 5511–5520.
[22] X. Zhang, N.V. Shirahatti, D. Mahadevan, S.H. Wright, A conserved glutamate residue in transmembrane helix 10 influences substrate specificity of rabbit OCT2 (SLC22A2), J. Biol. Chem. 280 (2005) 34813–34822.
[23] V. Gorboulev, N. Shatskaya, C. Volk, H. Koepsell, Subtype-specific affinity for corticosterone of rat organic cation transporters rOCT1 and rOCT2 depends on three amino acids within the substrate binding region, Mol. Pharmacol. 67 (2005) 1612–1619.
[24] M. Mueckler, C. Makepeace, Analysis of transmembrane segment 10 of the Glut1 glucose transporter by cysteine-scanning mutagenesis and substituted cysteine accessibility, J. Biol. Chem. 277 (2002) 3498–3503.
[25] Y. Huang, M.J. Lemieux, J. Song, M. Auer, D.N. Wang, Structure and mechanism of the glycerol-3-phosphate transporter from *Escherichia coli*, Science 301 (2003) 616–620.
[26] J. Abramson, I. Smirnova, V. Kasho, G. Verner, H.R. Kaback, S. Iwata, Structure and mechanism of the lactose permease of *Escherichia coli*, Science 301 (2003) 610–615.
[27] T. Hirai, S. Subramaniam, Structure and transport mechanism of the bacterial oxalate transporter OxlT, Biophys. J. 87 (2004) 3600–3607.
[28] M. Mueckler, C. Makepeace, Transmembrane segment 12 of the Glut1 glucose transporter is an outer helix and is not directly involved in the transport mechanism, J. Biol. Chem. 281 (2006) 36993–36998.
[29] M. Mueckler, C. Makepeace, Model of the exofacial substrate-binding site and helical folding of the human Glut1 glucose transporter based on scanning mutagenesis, Biochemistry 48 (2009) 5934–5942.